Long-range order produced by the interaction between spin waves in classical fcc Heisenberg models

Marko T. Heinilä* and Aarne S. Oja†
Low Temperature Laboratory, Helsinki University of Technology, 02150 Espoo, Finland‡
(Received 29 June 1993; revised manuscript received 27 August 1993)

Previous linear spin-wave calculations as well as Green's-function theories predict disorder at $T > 0$ for certain Heisenberg models in disagreement with the in-principle exact Monte Carlo simulations. In order to resolve this contradiction we extended the spin-wave theory beyond the usual Bloch's nonlinear approximation, including leading off-diagonal terms. We investigate the classical Heisenberg model on an fcc lattice for three pairs of coupling constants (J_1, J_2) which result in an infinite degeneracy for the magnetic ordering vector in the mean-field (MF) theory. We study in detail how the interaction between spin waves selects the ordering vector at the critical field between antiferromagnetic and paramagnetic phases. We find that the usually ignored nonlinear terms generate soft modes which are consistent with the order found by Monte Carlo simulations at zero field. We demonstrate the importance of these nonlinear effects by investigating antiferromagnetic models with a one- or two-dimensional degenerate MF manifold for the ordering vector. The model with the two-dimensional manifold seems ideal for a Monte Carlo study of domain growth in a first-order phase transition. Finally, we show that even when Bloch's nonlinear spin-wave theory gives qualitatively correct results, it can lead to a factor-of-three overestimate for the critical temperature of ferromagnetism. We find that this failure can be understood by considering the higher-order effects included in our extended spin-wave theory.

I. INTRODUCTION

In most Heisenberg systems the wave vector of magnetic order can be accurately predicted using the mean-field (MF) theory.[1] Under certain circumstances, however, the ordering vector shows an infinite degeneracy in the MF description. However, the degeneracy is partially lifted by thermal fluctuations which can even stabilize long-range order. Villain, *et al.*[2] discussed this surprising effect in the context of the Ising model and called it *ordering by disorder*. We study the details of this mechanism in Heisenberg models using nonlinear spin-wave theory and Monte Carlo simulations.

A well-known example of a system with a degenerate ordering vector in the MF theory is the antiferromagnetic nearest-neighbor Heisenberg model on a fcc lattice.[3–8] The linear spin-wave calculation of ter Haar and Lines[4] indicates diverging spin reduction $S - \langle S_z \rangle$ at finite temperatures. This has been taken as an indication of the absence of long-range order, both in classical and quantum systems. Similarly, Green's-function approaches[5] and, for example, the spherical model[9] predict no phase transition when $T > 0$. Monte Carlo simulations of classical systems[7,8] have recently shown, however, that thermal effects stabilize a type-I structure: Thus the models with a degenerate manifold provide a serious challenge to theories commonly used in studies of Heisenberg magnets.

There is clearly a need for an improved theory for understanding even classical systems in cases of ordering-vector degeneracy: This would facilitate the understanding of the in-principle exact Monte Carlo[7,8] results. To this end, we have formulated a spin-wave theory for the polarized paramagnetic phase of the classical fcc Heisenberg model with nearest-neighbor and next-nearest-neighbor exchange interactions. The classical spin vectors are converted into complex numbers using the Dyson-Maleev[10] transformation. The interaction between spin waves is treated using a diagrammatic method based on the use of the exact propagator. We obtain leading corrections to the classical limit of the conventional[11,12] nonlinear theory. By using these results we consider the models represented by exchange constants at the boundaries of the three principal kinds of antiferromagnetic structure[1] (I, II, III) and ferromagnetic order. Along three of the boundaries there is an infinite number of equivalent ordering vectors in the MF theory. We investigate the ordering process of these models by examining the softening[13] of spin-wave excitations in the paramagnetic phase above the critical field B_c at low temperatures. We find that at a finite temperature a soft mode appears for one of the wave vectors of the degenerate manifold.

The soft-mode wave vector found at $B_c(T)$, using our theory, gives correctly the order obtained in Monte Carlo simulations (Refs. 7 and 8 and Sec. III) at $B = 0$. As our theory is in agreement with the Monte Carlo results, our work elucidates the mechanism by which the interaction between spin waves stabilizes the long-range order. For example, at the boundary between the antiferromagnetic type-I and type-III structures ($J_1 > 0$, $J_2 = 0$), as well as between types II and III ($J_1 = 2J_2 > 0$), the degeneracy disappears when we include the leading contributions beyond the conventional, nonlinear spin-wave theory by Bloch.[11] For the nearest-neighbor model we find a type-

I soft mode: This is consistent with the order found in Refs. 7 and 8.

When $J_1 = 2J_2 > 0$ a soft mode appears for type-III order: a feature in accord with our Monte Carlo results (Sec. III A). Thus long-range order exists in this model in spite of the two-dimensional degenerate MF manifold. At the boundary of type-II and ferromagnetic spin configurations ($-J_1 = J_2 > 0$), we find, however, that the usual theory[11] is qualitatively correct, yielding ferromagnetic behavior: This is also in agreement with our Monte Carlo results (Sec. III B). The conventional calculation, however, overestimates T_c by a factor of 3. Our extended soft-mode theory shows that the higher-order contributions cannot be ignored in the region $T \gtrsim T_c^{\mathrm{MC}}$, thus explaining the reduction of T_c found in Monte Carlo simulations.

Our interest in this subject originates from our work to understand nuclear magnetic ordering of copper.[14] This fcc system, which orders antiferromagnetically in the nanokelvin regime, displays a near degeneracy of a set of ordering vectors. The magnetic phase diagram of copper has been investigated extensively, but one of the high-field phases still lacks an experimental characterization. The MF (Ref. 15) and linear spin-wave[13] theories have been used to predict the spin structure, but the role of spin-wave interactions in the selection of the ordering vector has not been investigated. The methods of the present work are not directly applicable to this problem because the interactions are highly anisotropic in copper. Quantum effects might also be important and more work is still needed to understand this interesting application.

The organization of the present paper is as follows. The classical soft-mode theory is formulated and applied for fcc Heisenberg magnets in Sec. II. The nonlinear soft-mode theory is constructed using classical Dyson-Maleev transformation in Sec. II B; the diagrammatic treatment of the spin-wave interaction is discussed in detail. Section II C presents the results of our extended theory and the usual nonlinear approach to three degenerate models; in Sec. III we study two of these models using a Monte Carlo simulation technique. Section IV concludes and summarizes our work.

II. CLASSICAL NONLINEAR SOFT-MODE THEORY

A. Classical Heisenberg model

We consider the Hamiltonian

$$\mathcal{H} = J_1 \sum_{j>i}^{\mathrm{NN}} \hat{\mathbf{S}}_i \cdot \hat{\mathbf{S}}_j + J_2 \sum_{j>i}^{\mathrm{NNN}} \hat{\mathbf{S}}_i \cdot \hat{\mathbf{S}}_j - \mathbf{B} \cdot \sum_i \hat{\mathbf{S}}_i \qquad (1)$$

for a classical spin model with an isotropic nearest-neighbor (NN) and next-nearest-neighbor (NNN) spin-spin exchange. Here $\hat{\mathbf{S}}_i$ denotes unit vectors on a fcc lattice with N sites and $\mathbf{B}$ is the external magnetic field. At $B = 0$ we find $\mathcal{H} = \frac{1}{2}\sum_{\mathbf{q}} \gamma_{\mathbf{q}} |\mathbf{S}_{\mathbf{q}}|^2$ where $\mathbf{S}_{\mathbf{q}} = N^{-1/2}\sum_i \hat{\mathbf{S}}_i \exp(i\mathbf{q}\cdot\mathbf{r}_i)$ and $\gamma_{\mathbf{q}} = \sum_i J_{ij}\exp(i\mathbf{q}\cdot\mathbf{r}_{ij})$. We obtain

$$\gamma_{\mathbf{q}} = 4(J_1 - 2J_2)(c_x c_y + c_y c_z + c_z c_x) + 4J_2(c_x + c_y + c_z)^2 - 6J_2, \qquad (2)$$

where $c_\nu = \cos(q_\nu a)$, $\nu = x, y, z$, and the lattice constant is $2a$. At zero temperature the spin structure of lowest energy is determined by minimizing $\gamma_{\mathbf{q}}$: Because of isotropy of the model defined by Eq. (1), one can always construct a helix using the minimum wave vector $\mathbf{Q}$ only. For a complete survey of this and related systems applying the mean-field theory, see Ref. 1. Realizations of this model among electronic magnets are summarized in Ref. 16. This approach could be relevant for nuclear magnets in the nanokelvin regime as well.[14,17]

The model Eq. (1) exhibits three examples of an infinite degeneracy of the ordering vector. For $J_1 > 0$, $J_2 = 0$ all vectors of the type $\mathbf{Q} = (\pi/a)(1, x, 0)$ are degenerate; this set includes, in particular, the antiferromagnetic (AF) type-I $[\mathbf{Q} = (\pi/a)(1,0,0)]$ and type-III $[\mathbf{Q} = (\pi/a)(1, \frac{1}{2}, 0)]$ structures. At the boundary of type-III and type-II $[\mathbf{Q} = (\pi/a)(\frac{1}{2}, \frac{1}{2}, \frac{1}{2})]$ orders with $J_1 = 2J_2 > 0$, we obtain a degenerate surface $c_x + c_y + c_z = 0$ for the ordering vector $\mathbf{Q}$. When $-J_1 = J_2 > 0$ the minimum is of the form $\mathbf{Q} = (\pi/a)(x, x, x)$, including type-II and ferromagnetic (F) spin alignments.

B. Classical spin-wave theory

We define the local frame $\{\hat{\mathbf{x}}_i, \hat{\mathbf{y}}_i, \hat{\mathbf{z}}_i\}$ of the spin site i in order to expand the spin vectors around a given configuration $\hat{\mathbf{S}}_i = \hat{\mathbf{z}}_i$. Using the spherical coordinates (θ_i, ϕ_i) we introduce complex quantities α_i by[18]

$$\begin{aligned}\hat{\mathbf{S}}_i^{\mathrm{HP}} &= \hat{\mathbf{z}}_i \cos\theta_i + \sin\theta_i(\hat{\mathbf{x}}_i \cos\phi_i + \hat{\mathbf{y}}_i \sin\phi_i) \\ &= \hat{\mathbf{z}}_i(1 - |\alpha_i|^2) + (1 - |\alpha_i|^2/2)^{1/2}(\hat{\mathbf{e}}_i \alpha_i^* + \hat{\mathbf{e}}_i^* \alpha_i),\end{aligned} \qquad (3)$$

where $\alpha_i = e^{i\phi_i}(1 - \cos\theta_i)^{1/2} = u_i + iv_i$ and $\hat{\mathbf{e}}_i = 2^{-1/2}(\hat{\mathbf{x}}_i + i\hat{\mathbf{y}}_i)$. Equation (3) is the classical version of the quantum mechanical Holstein-Primakoff[19] transformation. In statistical mechanics it is necessary to compute integrals over the solid angle of $\hat{\mathbf{S}}_i$. Owing to the relation $\sin\theta_i d\phi_i d\theta_i = 2du_i dv_i$ this can be converted to integration over the disk $|\alpha_i|^2 \le 2$. As in the quantum case, it is practical to remove the square root in Eq. (3) by writing

$$\hat{\mathbf{S}}_i^{\mathrm{DM}} = \hat{\mathbf{z}}_i(1 - |\alpha_i|^2) + \hat{\mathbf{e}}_i \alpha_i^* + (1 - |\alpha_i|^2/2)\hat{\mathbf{e}}_i^* \alpha_i \,. \qquad (4)$$

Here $\hat{\mathbf{S}}^{\mathrm{DM}}$ is a complex-valued vector analogous to a Dyson-Maleev[10] transformed quantum spin operator. A calculation[20] shows that

$$\int_0^{2\pi} (S_x^{\mathrm{DM}})^n (S_y^{\mathrm{DM}})^m d\phi = \int_0^{2\pi} (S_x^{\mathrm{HP}})^n (S_y^{\mathrm{HP}})^m d\phi \qquad (5)$$

for integers $n, m \ge 0$. Therefore, Eqs. (4) and (3) are equivalent in exact statistical calculations. Equation (5) shows explicitly that the imaginary part of $\hat{\mathbf{S}}^{\mathrm{DM}}$ does not survive the integration over the azimuthal angle ϕ_i: The agreement with the classical Holstein-Primakoff transfor-

mation, Eq. (3), is thus restored. Using Eq. (4) it is possible to avoid the tedious direct manipulation of the spherical coordinates (θ_i, ϕ_i) and the expansion of the square roots in Eq. (3).

An application of the transformation defined by Eq. (4) to the Hamiltonian of Eq. (1) yields

$$\mathcal{H} = E_0 + (B - \gamma_0)\sum_i |\alpha_i|^2 + \sum_{i,j} J_{ij}\alpha_i^*\alpha_j + \tfrac{1}{2}\sum_{i,j} J_{ij}(|\alpha_i|^2 - \alpha_i^*\alpha_j)|\alpha_j|^2 , \quad (6)$$

where $\mathbf{B} = B\hat{\mathbf{z}}$. The Fourier transformation

$$\alpha_i = \frac{1}{\sqrt{N}}\sum_{\mathbf{q}} \alpha_{\mathbf{q}} \exp(i\mathbf{q}\cdot\mathbf{r}_i) \quad (7)$$

defines the classical spin waves $\alpha_{\mathbf{q}}$. In terms of these the Hamiltonian emerges as

$$\mathcal{H} = E_0 + \mathcal{H}_2 + \mathcal{H}_4, \quad (8)$$

where E_0 is the energy of the parallel spin configuration, and

$$\mathcal{H}_2 = \sum_{\mathbf{q}} \epsilon_{\mathbf{q}} |\alpha_{\mathbf{q}}|^2, \quad (9)$$

$$\mathcal{H}_4 = \tfrac{1}{2}\sum_{\mathbf{q},\mathbf{1},\mathbf{2}} \Gamma(\mathbf{q};\mathbf{1},\mathbf{2})\, \alpha_{\mathbf{1}}^*\alpha_{\mathbf{2}}^*\alpha_{\mathbf{1}+\mathbf{q}}\alpha_{\mathbf{2}-\mathbf{q}}, \quad (10)$$

$$\epsilon_{\mathbf{q}} = B - \gamma_0 + \gamma_{\mathbf{q}}, \quad (11)$$

$$\Gamma(\mathbf{q};\mathbf{1},\mathbf{2}) = \frac{1}{N}[\gamma_{\mathbf{q}} - \tfrac{1}{2}(\gamma_{\mathbf{1}} + \gamma_{\mathbf{2}})], \quad (12)$$

where we have adopted the notation $\mathbf{k}_1 \equiv \mathbf{1}$, $\mathbf{k}_2 \equiv \mathbf{2}$. In quantum mechanical theory the Dyson-Maleev transformed Hamiltonian is non-Hermitian. Here, in analogy, $\mathcal{H}_4$ is a complex-valued quantity.

The Gibbs free energy G of the model Eq. (8) is given by

$$\beta G = -\ln\left[\int \exp(-\beta\mathcal{H}) \prod_{\mathbf{q}} d\,\mathrm{Re}\{\alpha_{\mathbf{q}}\}\, d\,\mathrm{Im}\{\alpha_{\mathbf{q}}\}\right] , \quad (13)$$

where $\beta = 1/T$ and temperature is defined by setting $k_B = 1$. The constraints $|\alpha_i|^2 \leq 2$ are abandoned: This is the approximation characteristic of conventional spin-wave theories, i.e., the neglect of the kinematical interaction.[3] The free energy G is expanded using a diagrammatic perturbation theory:

$$\beta(G - E_0) = -S_0 - \sum_{\mathbf{q}} \ln\frac{T}{\epsilon_{\mathbf{q}}} - \sum_{n=1}^{\infty} \frac{(-\beta)^n}{n!}\langle \mathcal{H}_4^n \rangle_c , \quad (14)$$

where S_0 is a constant depending on the normalization of the integrals in Eq. (13). The only nonzero pairwise averages of the quantities $\alpha_{\mathbf{1}}^*$, $\alpha_{\mathbf{2}}$ in the average $\langle\cdots\rangle_c$ are given by the free propagator $\langle|\alpha_{\mathbf{q}}|^2\rangle_0 = \int |\alpha_{\mathbf{q}}|^2 \exp(-\beta\mathcal{H}_2)/\int \exp(-\beta\mathcal{H}_2) = T/\epsilon_{\mathbf{q}}$; the subscript c reminds us that only the connected diagrams, here the terms proportional to N, appear in the average.

We wish to calculate the averages $\langle|\alpha_{\mathbf{q}}|^2\rangle = \delta G/\delta\epsilon_{\mathbf{q}}$ at a finite temperature. When the external field is lowered to the critical field $B_c(T)$ for antiferromagnetic ordering, a soft mode with $\langle|\alpha_{\mathbf{q}}|^2\rangle = \infty$ appears for the wave vector $\mathbf{q} = \mathbf{Q}$ characterizing the antiferromagnetic order immediately below $B_c(T)$.[13] Equation (14) is not adequate for studying the soft-mode transition at a finite T, because the expansion used is not well defined when $B_c(T) \leq B < B_c(0) = \gamma_0 - \min_{\mathbf{q}}\gamma_{\mathbf{q}}$, as $\epsilon_{\mathbf{q}}$ would assume negative values. Therefore, we cannot apply perturbation theory directly with $\mathcal{H}_2$, but we must replace it by an effective Gaussian Hamiltonian $\tilde{\mathcal{H}}_2$. To accomplish this we reorganize the series, writing

$$\mathcal{H} = \tilde{\mathcal{H}}_2 + \mathcal{V}, \quad (15)$$

$$\tilde{\mathcal{H}}_2 = \sum_{\mathbf{q}} \tilde{\varepsilon}_{\mathbf{q}} |\alpha_{\mathbf{q}}|^2 , \quad (16)$$

$$\mathcal{V} = \mathcal{H}_4 + \sum_{\mathbf{q}} \square_{\mathbf{q}} |\alpha_{\mathbf{q}}|^2 , \quad (17)$$

$$\square_{\mathbf{q}} = \epsilon_{\mathbf{q}} - \tilde{\varepsilon}_{\mathbf{q}} . \quad (18)$$

We replace $\mathcal{H}_2$ by $\tilde{\mathcal{H}}_2$ and $\mathcal{H}_4$ by $\mathcal{V}$ in Eq. (14). The function $\tilde{\varepsilon}_{\mathbf{q}}$ is defined by

$$\langle|\alpha_{\mathbf{q}}|^2\rangle = T/\tilde{\varepsilon}_{\mathbf{q}} . \quad (19)$$

On the other hand, the relation $\langle|\alpha_{\mathbf{q}}|^2\rangle = \delta G/\delta\square_{\mathbf{q}}$ allows one, when combined with Eq. (19), to solve for $\square_{\mathbf{q}}$:

$$\square_{\mathbf{q}} = -\Sigma_{\mathbf{q}}^{\mathrm{HF}} + T\left(\frac{\tilde{\varepsilon}_{\mathbf{q}}}{T}\right)^2 \sum_{n=2}^{\infty} \frac{(-\beta)^n}{n!}\langle \mathcal{V}^n |\alpha_{\mathbf{q}}|^2\rangle_c , \quad (20)$$

where the averages are calculated using the exact propagator $\langle|\alpha_{\mathbf{q}}|^2\rangle = T/\tilde{\varepsilon}_{\mathbf{q}}$. The quantity $\Sigma_{\mathbf{q}}^{\mathrm{HF}}$ is given by

$$\Sigma_{\mathbf{q}}^{\mathrm{HF}} = \frac{1}{N}\sum_{\mathbf{1}} (\gamma_0 - \gamma_{\mathbf{q}} - \gamma_{\mathbf{1}} + \gamma_{\mathbf{1}-\mathbf{q}})\frac{T}{\tilde{\varepsilon}_{\mathbf{1}}} . \quad (21)$$

Using Eq. (20) we can derive integral equations for a self-consistent determination of $\tilde{\varepsilon}_{\mathbf{q}}$. Noting that $\square_{\mathbf{k}} = O(\mathcal{H}_4)$ we iterate Eq. (20) until all $\square_{\mathbf{k}}$'s disappear from the right-hand side up to the desired order in $\mathcal{H}_4$. In the course of this calculation many of the terms in the expansion, i.e., reducible diagrams, cancel. The two lowest-order approximations obtained this way are

$$\tilde{\varepsilon}_{\mathbf{q}} = \epsilon_{\mathbf{q}} + \Sigma_{\mathbf{q}}^{\mathrm{HF}} + O(\mathcal{H}_4^2) , \quad (22)$$

$$\tilde{\varepsilon}_{\mathbf{q}} = \epsilon_{\mathbf{q}} + \Sigma_{\mathbf{q}}^{\mathrm{HF}} + \Sigma_{\mathbf{q}}^{(2)} + O(\mathcal{H}_4^3) , \quad (23)$$

where $\Sigma_{\mathbf{q}}^{(2)}$ is a six-dimensional integral,

$$\Sigma_{\mathbf{q}}^{(2)} = -T^2 \sum_{\mathbf{1},\mathbf{2}} [\Gamma(\mathbf{q}-\mathbf{2};\mathbf{1}+\mathbf{q},\mathbf{2})\Gamma(\mathbf{1};\mathbf{q},\mathbf{1}+\mathbf{2}) + \Gamma(\mathbf{1};\mathbf{1}+\mathbf{q},\mathbf{1}+\mathbf{2})\Gamma(\mathbf{1};\mathbf{q},\mathbf{2})](\tilde{\varepsilon}_{\mathbf{1}+\mathbf{q}}\tilde{\varepsilon}_{\mathbf{1}+\mathbf{2}}\tilde{\varepsilon}_{\mathbf{2}})^{-1} . \quad (24)$$

It is convenient to perform the derivations by defining suitable Feynman diagrams;[21] those contributing to $\Sigma_{\mathbf{q}}^{\mathrm{HF}}$ and $\Sigma_{\mathbf{q}}^{(2)}$ are shown in Fig. 1.

The nonlinear spin-wave theory based on Eq. (23) has not been studied before, at least not in explicit calculations. In contrast, Eq. (22) is the classical limit of a scheme known as the standard variational theory,[11] or as the spin-wave renormalization,[3] the second random-phase,[3] the Hartree-Fock (HF),[22] or the diagonal[12] approximation. As we will see, the theory based on Eq. (22) is not accurate enough for determining soft modes of the degenerate antiferromagnetic models of Sec. II A. In these cases the term $\Sigma_{\mathbf{q}}^{(2)}$ is decisive: Its omission would lead to qualitative disagreements between the spin-wave approach and the in-principle exact Monte Carlo calculations.

The diagrams included in a given approximation are defined by considering the expansion in terms of the free propagator $T/\epsilon_{\mathbf{q}}$. In order to find the diagrams summed in the theories like Eqs. (22) and (23), one must eliminate $\tilde{\varepsilon}_{\mathbf{q}}$ from $\langle|\alpha_{\mathbf{q}}|^2\rangle = T/\tilde{\varepsilon}_{\mathbf{q}}$ via successive applications of Eq. (22) or (23) and expansions of the denominators. One can then compare the series with the complete expansion $\langle|\alpha_{\mathbf{q}}|^2\rangle = \delta G/\delta\epsilon_{\mathbf{q}}$ where G given by Eq. (14).

Unfortunately, Eq. (23) is an integral equation for $\tilde{\varepsilon}_{\mathbf{q}}$ containing six-dimensional integrals over the first Brillouin zone. We are, therefore, led to introduce yet another approximative scheme in order to determine $\langle|\alpha_{\mathbf{q}}|^2\rangle$ beyond $\langle|\alpha_{\mathbf{q}}|^2\rangle^{\mathrm{HF}}$. We write

$$\tilde{\varepsilon}_{\mathbf{q}}^{\mathrm{HF}} = \epsilon_{\mathbf{q}} + \Sigma_{\mathbf{q}}^{\mathrm{HF}}, \tag{25a}$$

$$\tilde{\varepsilon}_{\mathbf{q}} = \tilde{\varepsilon}_{\mathbf{q}}^{\mathrm{HF}} + \Sigma_{\mathbf{q}}^{(2)}, \tag{25b}$$

where Σ^{HF} and $\Sigma_{\mathbf{q}}^{(2)}$ are calculated using $\tilde{\varepsilon}_{\mathbf{q}}^{\mathrm{HF}}$. The lack of self-consistency in Eq. (25b) discards a subset of the diagrams included in Eq. (23). Equation (25b) augments the Hartree-Fock theory, Eq. (25a), with the leading correction only. Nevertheless, the expansion of $\langle|\alpha_{\mathbf{q}}|^2\rangle = T/\tilde{\varepsilon}_{\mathbf{q}}$ in terms of the free propagator $T/\epsilon_{\mathbf{q}}$ contains all terms of the first and second order in $\mathcal{H}_4$ and a significant amount from all higher orders of the complete expansion. For the degenerate models of Sec. II A this is the lowest-order spin-wave theory which gives soft-mode behavior consistent with the accurate Monte Carlo simulations (Refs. 7 and 8 and Sec. III).

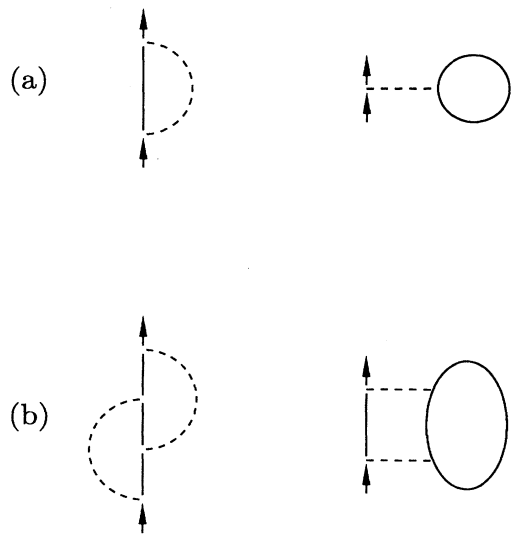

FIG. 1. Feynman diagrams contributing (a) to $\Sigma_{\mathbf{q}}^{\mathrm{HF}}$ and (b) to $\Sigma_{\mathbf{q}}^{(2)}$.

C. Soft-mode theory

Excitation of a $\mathbf{q} = \mathbf{0}$ spin wave corresponds to an overall rotation of the spins; it does not affect the exchange energy. The Zeeman energy will change, however, and one finds the exact result $\tilde{\varepsilon}_{\mathbf{0}} = B$. An inspection shows that $\Sigma_{\mathbf{0}}^{\mathrm{HF}} = \Sigma_{\mathbf{0}}^{(2)} = 0$, assuring that the treatment of the exchange energy is rotationally invariant. Therefore, we can solve Eq. (25a) by using the ansatz $\tilde{\varepsilon}_{\mathbf{q}}^{\mathrm{HF}} = B - \tilde{\gamma}_{\mathbf{0}} + \tilde{\gamma}_{\mathbf{q}}$ with $\tilde{\gamma}_{\mathbf{q}} = \sum_i \tilde{J}_{ij} \exp(i\mathbf{q}\cdot\mathbf{r}_{ij})$. The inverse Fourier transform of Eq. (25a) gives[23]

$$\tilde{J}_{ij} = J_{ij}\left\{1 + \frac{T}{N}\sum_{\mathbf{q}}\left[\exp(i\mathbf{q}\cdot\mathbf{r}_{ij}) - 1\right]/\tilde{\varepsilon}_{\mathbf{q}}^{\mathrm{HF}}\right\}, \tag{26}$$

allowing one to solve explicitly for the inverse mapping $J_{ij}(\{\tilde{J}_{ij}\}, T)$. Hence the effect of a finite temperature is, according to Eq. (25a), to modify the $T = 0$ spectrum $\epsilon_{\mathbf{q}}$ via a change of the nonzero coupling constants J_{ij} into the so-called "renormalized" values $\tilde{J}_{ij}(T)$.

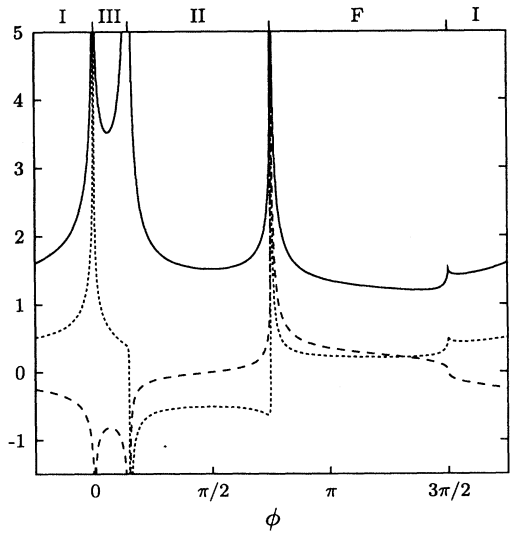

FIG. 2. Lattice Green's functions $G(1;\mathbf{r}_{ij})$ at the origin (solid curve), at the nearest-neighbor (dashed curve), and at the next-nearest-neighbor (dotted curve) lattice sites for $\tilde{J}_1 = \cos\phi$, $\tilde{J}_2 = \sin\phi$. The minima of $\tilde{\gamma}_{\mathbf{k}}$ are indicated by F and I–III, corresponding to ferromagnetism and the three principal kinds of antiferromagnetism on a fcc lattice, respectively.

It is convenient to express the integrals in Eq. (26) by means of functions $G(z;\mathbf{r}_{ij})$, known as lattice Green's functions[24] or generalized Watson's integrals:[25]

$$G(z;\mathbf{r}_{ij}) = \frac{1}{N}\sum_{\mathbf{q}} \frac{\exp(i\mathbf{q}\cdot\mathbf{r}_{ij})}{1 - z\tilde{\gamma}_{\mathbf{q}}/\tilde{\gamma}} , \qquad (27)$$

where $\tilde{\gamma} = \min_{\mathbf{q}} \tilde{\gamma}_{\mathbf{q}}$. The value $z = 1$ corresponds to $\tilde{\varepsilon}^{\mathrm{HF}}_{\mathbf{q}}$ with a soft mode and the interval $0 < z < 1$ to the ferro- or paramagnetic phase in an external field. The functions $G(1;\mathbf{r}_{ij})$ at the origin, the nearest-neighbor ($\mathbf{r}_1$) and at the next-nearest-neighbor ($\mathbf{r}_2$) lattice sites obtained by a numerical integration,[26] are shown in Fig. 2 as a function of the relative magnitude of the coupling constants $\tilde{J}_1$ and $\tilde{J}_2$. Note that $G(1;\mathbf{r}_{ij})$ diverges when $\tilde{J}_1 > 0$ and $\tilde{J}_2 = 0$, $\tilde{J}_1 = 2\tilde{J}_2 > 0$, or when $-\tilde{J}_1 = \tilde{J}_2 > 0$. At $J_1 = 0$ the model Eq. (1) reduces to four uncoupled simple cubic ferro- or antiferromagnets. The $B = 0$ transition temperature of the system Eq. (1) in the spherical approximation[9] is $T_c^{\mathrm{sph}} = T_c^{\mathrm{MF}}/G(1;\mathbf{0})$ where $\tilde{J}_{ij} = J_{ij}$ and T_c^{MF} is the mean-field result $T_c^{\mathrm{MF}} = -\min_{\mathbf{q}} \gamma_{\mathbf{q}}/(3k_B)$; T_c^{sph} is zero for the three degenerate models of Sec. II A.

The integrals $\Sigma^{(2)}_{\mathbf{q}}$ in Eq. (25b) can be calculated using an elementary Monte Carlo integration technique[27] with sufficient accuracy when the number of Monte Carlo points is on the order of 3×10^7; this is also enough for a good statistical error estimate. The soft-mode results for the three models of infinite degeneracy, discussed in Sec. II A, are summarized in Figs. 3(a)–3(c). When error bars are shown for $\tilde{\varepsilon}_{\mathbf{q}}$ they correspond to 95% statistical confidence interval of $\Sigma^{(2)}_{\mathbf{q}}$. The dashed lines in Figs. 3(a)–

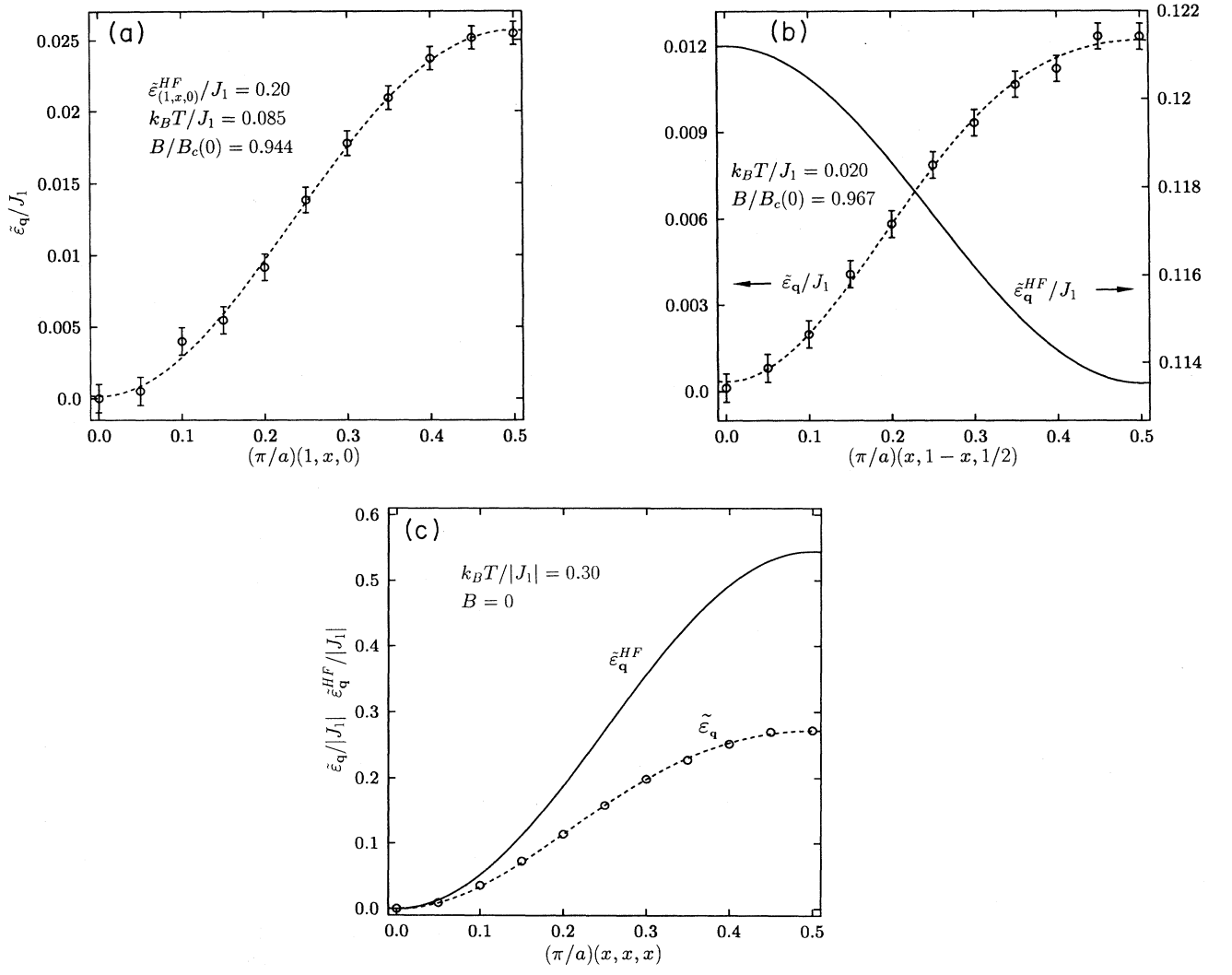

FIG. 3. Quantities $\tilde{\varepsilon}^{\mathrm{HF}}_{\mathbf{q}}$ and $\tilde{\varepsilon}_{\mathbf{q}}$, proportional to the inverses of the average excitation of the classical spin waves $\langle|\alpha_{\mathbf{q}}|^2\rangle$ given by Eqs. (25a) and (25b), along some zero-temperature degeneracy lines at the high-field (T,B) phase boundary (a) and (b) and at zero field (c). For boundary between (a) type I and type III, $J_1 > 0$, $J_2 = 0$; (b) type III and type II, $J_1 = 2J_2 > 0$; and (c) for type II and ferromagnetism, $-J_1 = J_2 > 0$.

3(c) are fits to the function $c_1 + c_2\cos(2\pi x) + c_3\cos(4\pi x)$ which is consistent with the periodicity of the $\mathbf{k}$ space.

We next discuss briefly the details of the soft-mode results for the three degenerate models of Sec. II A.

1. $J_1 > 0$, $J_2 = 0$

The solutions of Eqs. (25a)–(25b) are shown in Fig. 3(a) along the degeneracy line $\mathbf{q} = (\pi/a)(1, x, 0)$ for a representative point on the high-field phase boundary. There are no soft modes in the Hartree-Fock approximation, Eq. (25a), at finite temperatures. This is because it is not possible to remove the degeneration lines from $\tilde{\varepsilon}_{\mathbf{q}}^{\mathrm{HF}}$ by altering the coupling constant $\tilde{J}_1$ only: Functions $G(z; \mathbf{r}_{ij})$ diverge when $z \to 1$. In the extended theory Eq. (25b), however, a soft mode appears at $x = 0$, suggesting type-I order below $B_c(T)$. This result is consistent with the zero-field Monte Carlo simulations of Refs. 7 and 8.

The dashed line in Fig. 3(a) corresponds to an effective next-nearest-neighbor coupling $J_2^{\mathrm{eff}} \approx -0.006 J_1$. One might, therefore, suspect that the degeneracy affects the ordering vector when $0 < J_2 \lesssim 0.006 J_1$, thus stabilizing the type-I phase in a temperature interval immediately below T_N.

2. $J_1 = 2J_2 > 0$

The quantities $\tilde{\varepsilon}_{\mathbf{q}}^{\mathrm{HF}}$ and $\tilde{\varepsilon}_{\mathbf{q}}$ computed along the line $\mathbf{q} = (\pi/a)(x, 1-x, \frac{1}{2})$ are represented in Fig. 3(b). The minimum of $\tilde{\varepsilon}_{\mathbf{q}}^{\mathrm{HF}}$ is located at a type-II wave vector $(x = \frac{1}{2})$. One obtains this result also, for example, in the high-field approximation $z \ll 1$: $G(z; \mathbf{r}_{ij}) \approx z\tilde{J}_{ij}/\tilde{\gamma}$ for $\mathbf{r}_{ij} \neq \mathbf{0}$. Nevertheless, no soft mode appears in the HF theory. This can be seen by studying the cases when the real coupling constants J_1 and J_2 differ slightly from the degenerate values $J_1 = 2J_2 > 0$. In this case a soft mode forms at the minima of $\gamma_{\mathbf{q}}$. However, $\tilde{J}_1$ and $\tilde{J}_2$ renormalize toward the degenerate model. This follows from Eq. (26) together with the fact that the quantity $G(1; \mathbf{r}_1) - G(1; \mathbf{r}_2)$ is negative when $\tilde{J}_1 > 2\tilde{J}_2$ and changes its sign exactly at $\tilde{J}_1 = 2\tilde{J}_2$. One finds that functions $G(1; \mathbf{r}_{ij})$ diverge when $J_1 \to 2J_2 > 0$; i.e., zero-energy modes can appear at $T = 0$ only.

The inclusion of an off-diagonal contribution, Eq. (26), however, leads to the appearance of a soft mode at $x = 0$, corresponding to type-III order. The location of the soft mode was also confirmed by a study at a number of points elsewhere in the degeneracy plane $\cos(q_x a) + \cos(q_y a) + \cos(q_z a) = 0$. The location of the soft mode is consistent with zero-field Monte Carlo simulations of Sec. III A. These results suggest that the degenerate model with $J_1 = 2J_2 > 0$ has type-III long-range order in the thermodynamic limit.

3. $-J_1 = J_2 > 0$

The linear spin-wave theory for $T > 0$ at zero field gives the unphysical result $S - \langle S_z \rangle = \infty$ for a ferromagnetic structure because $G(1; \mathbf{0})$ diverges at the degeneration line. In another model with a diverging spin reduction, Rastelli, Sedazzari, and Tassi[22] have found that ferromagnetism is stabilized in the HF theory. Our model with $-J_1 = J_2 > 0$ shows quite similar behavior: Figure 3(c) illustrates $\tilde{\varepsilon}_{\mathbf{q}}$ and $\tilde{\varepsilon}_{\mathbf{q}}^{\mathrm{HF}}$ along the degeneracy line $\mathbf{q} = (\pi/a)(x, x, x)$. The soft mode forms at $\mathbf{q} = \mathbf{0}$ in both approximations, Eqs. (25a) and (25b). The error on the curve for $\tilde{\varepsilon}_{\mathbf{q}}$ is on the order of the size of the markers. The difference $G(1; \mathbf{r}_1) - G(1; \mathbf{r}_2)$ is in this case positive on both sides of the degeneration line: One finds, using Eq. (26), that temperature tends to stabilize a ferromagnetic structure when $-J_1 \approx J_2 > 0$. In this case, too, there is an agreement with Monte Carlo results; see Sec. III B.

The correction $\Sigma_{\mathbf{q}}^{(2)}$ could induce an antiferromagnetic instability causing $\min_{\mathbf{q}} \tilde{\varepsilon}_{\mathbf{q}} < 0$ around type-II wave vectors. According to the classical soft-mode theory, the instability occurs when $k_B T/|J_1| \approx 0.72$. Monte Carlo simulations of Sec. III B show, however, that the system is disordered above $k_B T_c/|J_1| \approx 0.65$ (see Fig. 5).

III. MONTE CARLO SIMULATIONS

The zero-field phase transition of the antiferromagnetic nearest-neighbor model has been studied in detail[6–8] by Monte Carlo (MC) simulations. A phase transition was observed in the first MC study[6] and it was proposed to be a consequence of an ordering by disorder mechanism. In more recent MC studies Minor and Giebultowicz,[7] as well as Diep and Kawamura,[8] found a discontinuous transition to a collinear type-I structure at $k_B T_N/J_1 \approx 0.45$. We too have investigated the nearest-neighbor model. Our Monte Carlo studies on this model agree well with the findings of Refs. 7 and 8. The type-I order of this model is therefore established by three independent Monte Carlo calculations. Below we report results of our simulations of the two other degenerate models with next-nearest-neighbor exchange.

A. Monte Carlo simulation of the model with $J_1 = 2J_2 > 0$

We employ the heat bath[28] Monte Carlo method of Ref. 29. The runs were started with a random spin configuration at a temperature well within the paramagnetic phase. Temperature was then lowered exponentially by using 3% steps. At each temperature, 6000 Monte Carlo updates per spin (MCS) were performed; estimates for the thermodynamic quantities were obtained as averages over the last 4000 MCS. Eventually, a discontinuous transition to an ordered state took place. Similar runs were made for increasing temperature as well. The initial configurations for them were the structures obtained deep in the ordered state during the cooling runs.

The internal energy $E = \langle \mathcal{H} \rangle$ calculated in these runs is shown in Fig. 4(a). The statistical error is smaller than the size of the symbols: Because of large overlap, all data points are not shown. The salient feature of the

results is the pronounced hysteresis loop which is of the same order of magnitude as T_N. The size effect between $N = 4096$ and $N = 8000$ in internal energy is difficult to notice on the scale of Fig. 4(a). However, for $N = 1728$ the points deviate from the others in the paramagnetic phase, and the lower transition temperature also appears to be higher than for $N = 4096$ and $N = 8000$.

In the ordered structure found in the runs for $N = 4096$ and 8000, the type-III Fourier component was clearly predominant. The spin structure was identified as the simple collinear[30–32] type-III[33,3] configuration

$$\hat{\mathbf{S}}_i = \hat{\mathbf{u}}\sqrt{2}\cos\left[\frac{\pi}{a}(1,\tfrac{1}{2},0)\cdot\mathbf{r}_i + \frac{\pi}{4}\right], \tag{28}$$

where $\hat{\mathbf{u}}$ is a unit vector. For $N = 1728$, however, the low-temperarature state was a complicated mixture of various Fourier amplitudes, degenerate in the mean-field level.

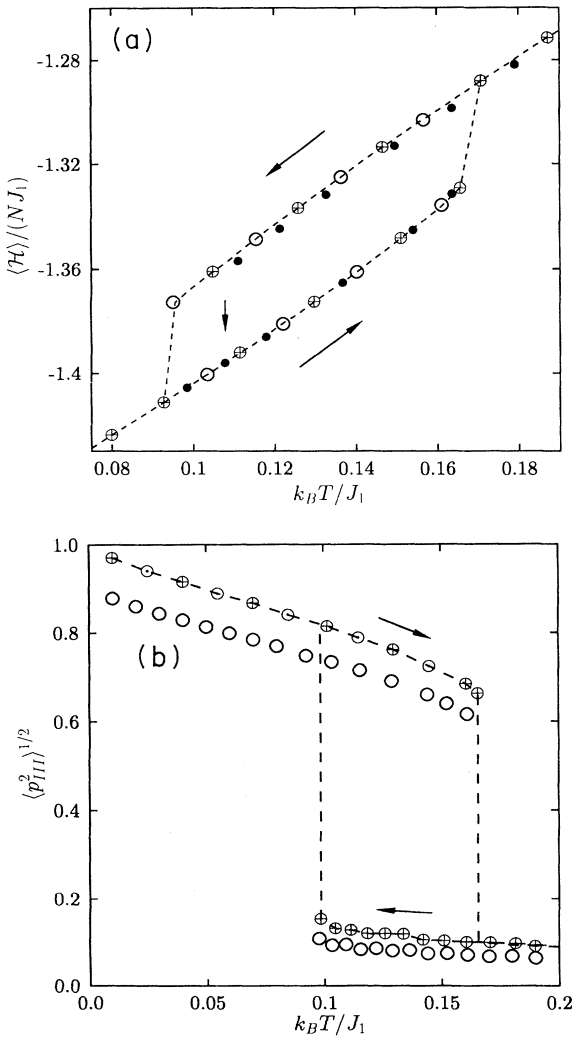

FIG. 4. (a) Internal energy $\langle\mathcal{H}\rangle$ obtained in Monte Carlo simulations of the model $J_1 = 2J_2 > 0$ at zero field. (b) The type-III Fourier amplitude $\langle p^2_{\rm III}\rangle^{1/2}$. Symbols denote system sizes of $N = 1728$ (●), 4096 (⊕), and 8000 (○, ⊙). The dashed lines are guides for the eyes. In (a) the vertical arrow indicates the transition point to the low-temperature phase in the run with $N = 1728$.

We define the quantity $p^2_{\rm III}$ by

$$p^2_{\rm III} = \sum_{\mathbf{Q}}^{\rm III}\left|\frac{1}{N}\sum_i \hat{\mathbf{S}}_i \exp(i\mathbf{Q}\cdot\mathbf{r}_i)\right|^2, \tag{29}$$

where the $\mathbf{Q}$ sum is taken over the six inequivalent type-III wave vectors. The mean-square Monte Carlo average $\langle p^2_{\rm III}\rangle^{1/2}$ is shown in Fig. 4(b). The points denoted by ⊕ and ○ were obtained from the runs of Fig. 4(a). An additional run (⊙), started with a perfect collinear type-III configuration, was performed with decreasing temperature. The values ○ ($N = 8000$) are clearly smaller than those with ⊕ ($N = 4096$). This is due to defects formed during cooling from the paramagnetic phase because the data points ⊙ ($N = 8000$) and ⊕ agree. A tendency for formation of defects was also reported in Refs. 7 and 8 for the model with $J_1 > 0$, $J_2 = 0$.

The Monte Carlo data for $N = 8000$ was checked by using a 2-times-slower annealing rate with 12000 MCS between 3% changes in temperature. The results agreed well with the ○'s of Figs. 4(a) and 4(b). However, for $N = 4096$ the 2-times-slower annealing rate produced defective type-III structures with $\langle p^2_{\rm III}\rangle^{1/2} \approx 0.74$ at $k_BT/J_1 = 0.01$, and the cooling phase transition appeared to take place a few temperature steps earlier than in faster runs. This suggests that at this annealing rate size effects can be still observed in the ordering process when $N = 4096$.

1. *Relaxation rate of* $p^2_{\rm III}$

In order to ensure that our MC runs are long enough, we have studied the normalized autocorrelation function[34]

$$\phi[A](t) = \frac{\langle A(t_0)A(t_0+t)\rangle - \langle A\rangle^2}{\langle A^2\rangle - \langle A\rangle^2}. \tag{30}$$

The relaxation time of the quantity A is defined by[34]

$$\tau[A] = \int_0^\infty \phi[A](t)dt. \tag{31}$$

Because the slowest relaxing quantity is the order parameter $p^2_{\rm III}$, it is necessary to consider $\phi[p^2_{\rm III}](t)$. We have studied this function at $k_BT/J_1 = 0.13$ for a system with $N = 4096$ using runs of 2.5×10^5 MCS, both in the paramagnetic and in the type-III phase. Obviously one of the phases has to be metastable but both survived during the entire simulation. The long-time tail $\phi[p^2_{\rm III}](t) < 0.1$ turned out to be difficult to determine accurately: Ignoring its contribution to the relaxation time we find $\tau[p^2_{\rm III}] \approx 81$ MCS and $\tau[p^2_{\rm III}] \approx 21$ MCS for the paramagnetic and type-III phases, respectively. For exponential relaxation these estimates would be 90% of the correct result.

2. T_N

We have determined the location of T_N by the method proposed by Creutz, Jacobs, and Rebbi.[35,36] One-half of the $N = 8000$ lattice was initially set to the paramagnetic phase and the other to the type III ordered configuration. The halves were taken from separate samples of type-III phase and disordered paramagnetic structure which were equilibriated by simulation of 4000 MCS. The stable phase with lower free energy soon replaced the metastable half if simulation was done far from T_N. We found that the phase interface is always unstable and that the system collapsed to one of the bulk phases in less than 1000 MCS. Several runs suggested that $0.148 < k_BT_N/J_1 < 0.1505$. In this temperature interval the final spin configuration can be of type III as well as paramagnetic when $N = 8000$. We carried out 10 runs at $k_BT/J_1 = 0.1505$ and we detected the paramagnetic phase as the final phase 8 times and the type-III structure 2 times. In 10 runs at $k_BT/J_1 = 0.148$ we found 9 times the type-III phase and once the paramagnetic state.

B. Monte Carlo simulation of the model with $-J_1 = J_2 > 0$

Monte Carlo estimates for the mean-square spontaneus magnetization $\langle m^2\rangle^{1/2}$, where $m^2 = |N^{-1}\sum_i \hat{\mathbf{S}}_i|^2$, are shown in Fig. 5. The results were obtained by initializing the runs in the paramagnetic phase with a random spin configuration; the temperature was then reduced gradually. The ferromagnetic tendency is clear. Approximating T_c by the inflection point of the magnetization we obtain $k_BT_c/|J_1| \approx 0.65$. Type-II order did not appear in any of the cooling runs.

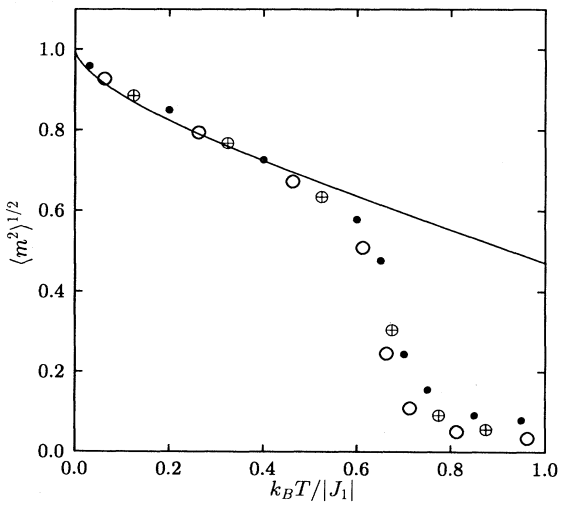

FIG. 5. Mean-square average magnetization $\langle m^2\rangle^{1/2}$ in the model $-J_1 = J_2 > 0$. The symbols denote system sizes $N = 1728$ (●), 4096 (⊕), and 8000 (○). The solid line is the spontaneous magnetization calculated using the HF spin-wave theory.

The solid line in Fig. 5 is the magnetization calculated using the usual HF spin-wave theory. According to this approach the maximum temperature for a nonzero magnetization is $k_BT_c^{SW}/|J_1| \approx 1.8$, in close agreement with the mean-field result $k_BT_c^{MF}/|J_1| = 2$. The Monte Carlo estimate $k_BT_c/|J_1| \approx 0.65$ reveals a gross failure of these theories. However, the temperature $k_BT/|J_1| = 0.72$ for type-II instability against ferromagnetism in our extended soft-mode theory agrees quite well with T_c. The Monte Carlo result of Fig. 5 shows that the off-diagonal contributions are not enough to stabilize a type-II phase. These corrections could, however, have a crucial role together with the features ignored in our idealized classical model. EuSe (Refs. 37 and 16) provides an experimental system with $-J_1 \approx J_2 > 0$, but in this case lattice distortions have been proposed to be important.[37]

The low-temperature magnetization is not a linear function of T which manifests the failure of the linear spin-wave theory. The quantum mechanical analog of this effect was discussed in Ref. 22.

IV. SUMMARY

Three models of an infinite wave-vector degeneracy in the mean-field theory were investigated in the context of the classical Heisenberg model with nearest-neighbor and next-nearest-neighbor exchange interactions on a fcc lattice. Using the classical Dyson-Maleev formalism the soft-mode approach for isotropic classical systems was extended beyond the nonlinear theory of Bloch[11] by inclusion of a high-order off-diagonal contribution caused by the dynamical[10] interaction between the classical spin waves.

We have shown that our extended soft-mode theory, unlike the conventional method, correctly predicts the zero-field order found in Monte Carlo simulations of the degenerate models. Our calculations indicated, in particular, that a soft mode corresponding to type-I order forms in the high-field paramagnetic phase of the antiferromagnetic nearest-neighbor model,[38] thus suggesting that the type-I order found in the Monte Carlo simulations of Refs. 7 and 8 is present in the thermodynamic limit as well.

The fcc Heisenberg model with $J_1 = 2J_2 > 0$, exhibiting a two-dimensional manifold of wave vectors degenerate in the mean-field theory, was studied in detail. The extended soft-mode approach showed type-III order, and this conclusion was also confirmed by zero-field Monte Carlo simulations which indicated collinear[30–32] type-III order. A similar structure has been found previously for a model without degeneracy ($J_1 = 10J_2 > 0$).[33] The effect of the degenerate manifold is, however, to suppress the Néel temperature down to $T_N = 0.15 \times T_N^{MF}$. The first-order nature of the zero-field phase transition in this model was found to be very strong with a well-defined hysteresis. The quite large ground-state degeneracy does not destroy the long-range order as happens, for example, in an even more frustrated three-dimensional model studied in Ref. 39.

Finally, we studied a model with a zero-temperature

degeneration line between ferromagnetic and type-II wave vectors. Bloch's nonlinear theory predicted ferromagnetism in agreement with the Monte Carlo result. We found, however, that in order to understand the reduction of T_c by a factor of 3 in Monte Carlo simulations from the Bloch's theory and the mean-field results it was necessary to consider the higher-order effects included in our extended spin-wave theory. We found that off-diagonal contributions tend to stabilize a type-II phase, but this tendency is not strong enough in order to make the type-II phase appear.

Note added in proof. The presented calculations for the models with $J_1 > 0$, $J_2 = 0$, and $J_1 = 2J_2 > 0$ do not exclude the possibility that the low-temperature phase when $0 < B < B_c$ could be different from both the phase obtained in MC simulations at $B = 0$ and that suggested by the soft-mode theory in the high-field paramagnetic region. Our annealing simulations (unpublished) of the model with $J_1 > 0$, $J_2 = 0$ suggest, however, that for this case the model exhibits type-I order in all fields $B < B_c$, and that the spin configurations are qualitatively similar to those obtained by us in Ref. 32 for a model with $J_1 = -10J_2 > 0$. However, our recent MC simulations (unpublished) for the model with $J_1 = 2J_2 > 0$ in nonzero fields suggest more complicated behavior.

ACKNOWLEDGMENTS

We thank O.V. Lounasmaa and P.I. Soininen for useful discussions. This work was supported by the Academy of Finland and by the Magnus Ehrnrooth Foundation (M.T.H.).

* Electronic address: Marko.Heinila@hut.fi
† Electronic address: Aarne.Oja@hut.fi
‡ FAX: +358-0-451-2969

[1] J.S. Smart, *Effective Field Theories of Magnetism* (Saunders, Philadelphia, 1966).
[2] J. Villain, R. Bidaux, J.-P. Carton, and R. Conte, J. Phys. (Paris) **41**, 1263 (1980).
[3] F. Keffer, in *Encyclopedia of Physics — Handbuch der Physik*, Vol. XVIII/2, edited by S. Flügge (Springer-Verlag, Berlin, 1966).
[4] D. ter Haar and M.E. Lines, Philos. Trans. R. Soc. London A **255**, 1 (1962). See also M.E. Lines, Proc. R. Soc. London **271**, 105 (1963).
[5] For example, see M.E. Lines, Phys. Rev. **135**, A1336 (1964); **139**, A1304 (1965).
[6] J.F. Fernández, H.A. Farach, C.P. Poole, Jr., and M. Puma, Phys. Rev. B **27**, 4274 (1983).
[7] W. Minor and T.M. Giebultowicz, J. Phys. (Paris) Colloq. **49**, C8-1551 (1988).
[8] H.T. Diep and H. Kawamura, Phys. Rev. B **40**, 7019 (1989).
[9] T.H. Berlin and M. Kac, Phys. Rev. **86**, 821 (1952). For a discussion, see Ref. 12, Vol. 2. Note that $T_c^{\text{Heisenberg}} = \frac{1}{3}T_c^{\text{Ising}}$ in spherical approximation for given J_{ij}'s.
[10] F.J. Dyson, Phys. Rev. **102**, 1217 (1956); **102**, 1230 (1956); S.V. Maleev, Zh. Eksp. Teor. Fiz. **33**, 1010 (1957) [Sov. Phys. JETP **64**, 654 (1958)].
[11] M. Bloch, Phys. Rev. Lett. **9**, 286 (1962).
[12] D.C. Mattis, *The Theory of Magnetism* (Springer-Verlag, Heidelberg, 1981 and 1985), Vols. 1 and 2.
[13] A.S. Oja and H.E. Viertiö, Phys. Rev. B **47**, 237 (1993).
[14] For a recent review, see P.J. Hakonen, O.V. Lounasmaa, and A.S. Oja, J. Magn. Magn. Mater. **100**, 394 (1991).
[15] H.E. Viertiö and A.S. Oja, Phys. Rev. B **48**, 1062 (1993).
[16] M.S. Seehra and T.M. Giebultowicz, Phys. Rev. B **38**, 11898 (1988).
[17] P.J. Hakonen, R.T. Vuorinen, and J.E. Martikainen, Phys. Rev. Lett. **70**, 2818 (1993).
[18] For a review on various transformations of quantum spin operators and their derivation, see Ref. 12.
[19] J. Holstein, and N. Primakoff, Phys. Rev. **58**, 1908 (1940). For a review, see Ref. 3.
[20] Successive partial integrations using relations $\partial_\phi S_x = -S_y$ and $\partial_\phi S_y = S_x$, valid for both HP and DM, reduce both sides of Eq. (5) to zero if n and m are not both even. Otherwise, one finds $\int (S_x^{\text{DM}})^{2l} = \int (S_x^{\text{HP}})^{2l}$ which can be established by a direct evaluation of the integrals.
[21] See, for example, A.L. Fetter and J.D. Walecka, *Quantum Theory of Many-Particle Systems* (McGraw-Hill, New York, 1971).
[22] E. Rastelli, S. Sedazzari, and A. Tassi, J. Phys. Condens. Matter **3**, 5861 (1991).
[23] For an analogous result for $S = \frac{1}{2}$, see L.P. Horwitz and D.C. Mattis, Phys. Rev. Lett. **10**, 511 (1963).
[24] Green's functions for various lattices, see, for example, R. Friedberg and O. Martin, J. Phys. A **20**, 5095 (1987); J. Hoshen, and R. Kopelman, J. Math. Phys. **17**, 2067 (1976); M. Inoue, *ibid.* **15**, 704 (1974); G.S. Joyce, J. Phys. A **5**, L65 (1972).
[25] We quote the results for $G(z;\mathbf{r}_{ij})$ obtained by G.N. Watson, Q. J. Math. (Oxford) **10**, 266 (1939): $G(1;\mathbf{0}) = 1.3446611832$ for $\tilde{J}_1 < 0$, $\tilde{J}_2 = 0$, and $G(1;\mathbf{0}) = 1.5163860592$ for $\tilde{J}_1 = 0$, $\tilde{J}_2 \neq 0$.
[26] We employed an adaptive scheme based on the tetrahedron formulas of J. Rath, and A.J. Freeman, Phys. Rev. B **11**, 2109 (1975).
[27] See, for example, W.H. Press, S.A. Teukolsky, W.T. Vetterling, and B.P. Flannery, *Numerical Recipes in C*, 2nd ed. (Cambridge University Press, Cambridge, England, 1992), p. 304. The pseudo-random numbers were generated by using one of the algorithms (RCARRY) studied in the review F. James, Comput. Phys. Commun. **60**, 329 (1990).
[28] The so-called heat bath approach, described (e.g.) in Ref. 29, is faster but equivalent to (e.g.) the Metropolis method; for a general discussion, see J.W. Negele and H. Orland, *Quantum Many-Particle Systems* (Addison-Wesley, Reading, MA, 1988), p. 408.
[29] S.J. Frisken and D.J. Miller, Phys. Rev. Lett. **61**, 1017 (1988).
[30] C.L. Henley, J. Appl. Phys. **61**, 3962 (1987).
[31] C.L. Henley, Phys. Rev. Lett. **62**, 2056 (1989).
[32] M.T. Heinilä and A.S. Oja, Physica B (to be published).

[33] T.M. Giebultowicz and J.K. Furdyna, J. Appl. Phys. **57**, 3312 (1985).
[34] K. Binder and D.W. Heerman, *Monte Carlo Simulation in Statistical Physics* (Springer-Verlag, Berlin, 1988).
[35] M. Creutz, L. Jacobs, and C. Rebbi, Phys. Rev. D **20**, 1915 (1979).
[36] D. Auerbach, E. Domany, and J.E. Gubernatis, Phys. Rev. B **37**, 1719 (1988).
[37] H. Callen and M.A. de Moura, Phys. Rev. B, **16**, 4121 (1977).
[38] According to Ref. 8 the type-I order in the $J_1 > 0$, $J_2 = 0$ model was also anticipated by C.L. Henley (Ref. 30). However, Henley discussed in his paper only systems with $J_2 < 0$ or $J_2 > 0$, using the classical linear spin-wave theory. No reference was made to the degenerate $J_2 = 0$ model. Henley's arguments (Refs. 30–32) give the local geometry of the spin structure (e.g., collinearity), but not the ordering vector itself. When $T > 0$ the linear spin-wave theory gives an unphysical, diverging spin reduction (Ref. 4).
[39] J.N. Reimers, Phys. Rev. B **45**, 7287 (1992).